Transactions of the 17th International Conference on Structural Mechanics in Reactor Technology (SMiRT 17)
Prague, Czech Republic, August 17 –22, 2003

Paper # D04-4

Application of the Seebeck effect for the monitoring of neutron embrittlement and low-cycle fatigue in nuclear reactor technology

M. Niffenegger[1], K. Reichlin[1] and D. Kalkhof[1]
[1)] Paul Scherrer Institut, CH-5232 Villigen PSI, Switzerland

ABSTRACT

The monitoring of neutron embrittlement and low-cycle fatigue in nuclear reactor steel is an important topic in lifetime extension of nuclear power plants. We therefore investigated the application of the Seebeck effect for determining material degradation of common reactor pressure vessel (RPV) steel. The Seebeck coefficients (SC) of several irradiated Charpy specimens made from Japanese JRQ-steel were measured. The specimens suffered a fluence from 0 up to 4.5 E^{19} neutrons per cm^2 with energies higher than 1MeV.

The measured changes of the SC within this range were about 500 nV, increasing continuously in the range under investigation. Some indications of saturation appeared at fluencies larger than 4.5 E^{19} neutrons per cm^2. We obtained a linear dependency between the SC and the temperature shift . T_{41} of the Charpy energy vs. temperature curve which is widely used to characterize material embrittlement. Similar measurements were performed on specimens made from the austenitic stainless steel X6CrNiTi18-10 (according to DIN 1.4541) that were fatigued by applying a cyclic strain amplitude of 0.28%.

Further investigations were made to quantify the size of the gauge volume in which the termoelectric power is generated. It appeared that the information gathered from a Thermo Electric Power (TEP) measurement is very local. To overcome this problem we propose a novel TEP-method using a Thermoelectric Scanning Microscope (TSM).

We finally conclude that the change of the SC has a potential for monitoring of material degradation due to neutron irradiation and thermal fatigue, but it has to be taken into account that several influencing parameters could contribute to the TEP in either an additional or extinguishing manner. A disadvantage of the method is the requirement of a clean surface without any oxide layer. This disadvantage can partially be avoided by using the proposed new TSM.

KEY WORDS: thermoelectricity, monitoring of material degradation, neutron irradiation induced embrittlement, thermal fatigue, non-destructive testing, diagnostics, nuclear reactor pressure vessel steel, Seebeck effect, ductile to brittle transition zone.

INTRODUCTION

Monitoring of material degradation of low-alloy ferritic reactor pressure vessel steel (LAS) is still an unsolved problem. Especially material embrittlement caused by neutron irradiation is an important topic revived by the desire for lifetime extension of nuclear power plants.

One physical effect that might be used for the detection of material degradation is the Seebeck effect. The fact that a heat flow is accompanied by a small electric current, discovered 1821 by Thomas Seebeck, is one of several thermoelectric effects and mainly used for measuring temperatures with thermocouples (TC) [1]. The generated electric field is proportional to the temperature gradient whereby the proportionality factor is called Seebeck coefficient (SC). We summarize the main equations coming from the theory of thermoelectricity which are essential to understand the origin of the TEP. A more detailed derivation of the theory of thermoelectricity is given in reference [2].

It is well known by producers of TC's that the material dependent SC is not a constant, but might change due to several influences, leading to a drift of the TEP [3-6]. One of these error sources is the irradiation by neutrons that occurs in nuclear power plants or in the target of a neutron spallation source. Other influencing parameters are e.g. heat treatments and plastic deformations. However, if the change of SC is a well-defined function of the neutron fluence and if the effect is large enough compared with that of other influencing parameters, it could be used for monitoring of material embrittlement which in the case of RPV is correlated to the neutron fluence. First investigations concerning this application were performed within the framework of the European network AMES (Ageing Materials Evaluation and Studies) by EDF [7] and JRC Petten [8]. Their results were encouraging enough to justify the TEP-method at PSI. For this purpose we used the TEP-device developed by the Institut National des Sciences Appliquées de Lion (INSA).

In order to clarify the application of the TEP-method to neutron embrittlement of LAS we measured the SC of a set of irradiated Charpy specimens made from the Japanese RPV-material JRQ [9].

Further, we investigated the change of the SC due to fatigue cycles on a set of specimens made from austenitic stainless steel that suffered different numbers of load cycles with a total strain amplitude $\varepsilon_t/2$ of 0.28 %. We compared the results of these measurements with other material characteristics e.g. with the martensitic content.

For physical reasons the information gained by a TEP-measurement is limited to a rather small gauge volume near the heat source. In order to get an idea of the size of the gauge volume, we made extensive calculations by means of the finite element method (FEM).

In general our first investigations are very promising, especially the application of TEP-measurements for monitoring neutron embrittlement. However, we propose a novel TEP-measuring method that we call Thermoelectric Scanning Microscope (TSM) with the potential to improve the information about inhomogeneous material degradation.

THE SEEBECK EFFECT

In solids, heat is transported by phonons and free electrons. For metals, the main contribution to thermal conduction stems from the electrons. Electrons are therefore carriers of both, thermal energy and electric charge. That means: thermal and electric currents are coupled phenomena with the consequence, that an electric current accompanies a heat flow. This is the origin of the Seebeck effect whose manifestation is a thermoelectric voltage. In the theory of thermoelectricity this voltage can be derived starting with the Boltzmann equations, either by introducing a quantum mechanical probability function or as it is common practice, by using the so-called relaxation time ansatz for the time derivation of the electron distribution function from the Fermi distribution and assuming a spherical Fermi surface. A detailed theoretical derivation is given in [2]. However, we here only emphasize the results of the theory, some of its practical aspects and interpretations.

The important results of the thermoelectric theory are the two coupled equations (1) and (2) for the electrical j_E and thermal current j_Q as a function of their origins, electric field $\boldsymbol{\varepsilon}$ and thermal gradient dT/dx.

$$j_E = L^{11}\boldsymbol{\mathcal{E}} + L^{12}\left(-dT/dx\right) \tag{1}$$

$$j_Q = L^{21}\boldsymbol{\mathcal{E}} + L^{22}\left(-dT/dx\right) \tag{2}$$

Equations (1-2) describes both, the Seebeck and the Peltier effect. From Eq. (1) we get for j_Q=0, i.e., if we measure the electric potential using a high resistance voltmeter (j_E=0), the electric field inside the metal:

$$\boldsymbol{\mathcal{E}}_x = \left(L^{11}\right)^{-1}\left(L^{12}\right)\frac{\cdot T}{\cdot x} = K(T)\frac{\cdot T}{\cdot x} \tag{3}$$

This is known as the Seebeck effect. For an applied electric field and a vanishing temperature gradient we get from Eq. (1) and Eq. (2) the equations for the thermal and electrical current:

$$j_Q = L^{21}\boldsymbol{\mathcal{E}} \qquad \text{and} \qquad j_E = L^{11}\boldsymbol{\mathcal{E}} \tag{4}$$

that can be summarized to

$$j_Q = L^{21}\left(L^{11}\right)^{-1} j_E \qquad \text{or} \qquad j_E = L^{11}\left(L^{21}\right)^{-1} j_Q \tag{5}$$

where the coefficient $L^{21}\left(L^{11}\right)^{-1} =: .$ is the so called Peltier coefficient. The thermoelectrical potential difference U (thermoelectric voltage or thermoelectric power TEP) between two points 0 and l of a specimen is

$$U = \int_0^l \boldsymbol{\mathcal{E}}(x)dx = \int_0^l dx K(T,x)\frac{\cdot T}{\cdot x} = \int_{T_0}^{T_1} K(T,x)\ dT = \overline{K}(T_1 - T_0) \tag{6}$$

where the mean Seebeck coefficient $\overline{K}$ is

$$\overline{K} = \frac{1}{(T_1 - T_0)}\int_{T_0}^{T_1} K(T,x)\ dT \tag{7}$$

or because T is a function of the space coordinate x

$$\overline{K} = \frac{1}{(T_1 - T_0)}\int_0^l K(T,x)\ \frac{dT}{dx}dx \cdot \tag{8}$$

Equation (6) expresses that the TEP U, which is generated between two points, is proportional to the temperature difference between these points whereas the proportionality factor is the mean Seebeck coefficient $\overline{K}$. However, it is essential to realize that the TEP is generated only in the area with a non-vanishing temperature gradient. Further, if

the two points are at the same temperature (T_0=T_1) as in a closed loop, the integral (6) is zero in a homogeneous (K(x)= constant) material. However, in an inhomogeneous material, where K(x) is an explicit function of x, we will get a thermoelectric voltage U even T_0=T_1, as far as the temperature on the integration path is not constant. Based on these properties of equation (6) we can determine $\overline{K}$ from a measurement of the TEP by applying a temperature gradient over a specimen. $\overline{K}$ can be used to characterize the change of the mean material property, i.e. embrittlement of the material due to neutron irradiation.

If we scan the specimen by moving a local temperature gradient along the specimen's surface, we can detect localized inhomogeneities in the material by measuring U according to Eq. (6).

MEASUREMENTS OF THE TEP

Experimental set-up

To experimentally verify the application of the SC for material characterization we used a special equipment that allows to apply a temperature difference on Charpy specimens and to measure the resulting thermoelectric power. The instrumentation of the used TEP-device developed by INSA de LYON consists of two parts. One part is used to apply the temperature gradient on the specimen and to measure both, temperatures and TEP. This device can be operated in hot cells. The second part acquires the data and is an easy to use control instrument that can be put outside the hot cell.

The specimens can be fixed on two supports made of copper by a pneumatic piston with constant pressure in order to guarantee two contact lines. These contact lines are held on two different temperatures fixed at 15°C and 25°C, respectively, in our experiments. The two temperatures are measured by thermocouples mounted under the contact surface of the support. The operating conditions are controlled by internal Peltier elements, cooling water, platinum resistance sensors and resistant heating within an accuracy of +/- 0.1°C. After stabilizing the system, the measured TEP is read out and displayed on the screen. The amplifier for the thermoelectric voltage has a resolution of 5 nV and is characterized with an excellent stability due to temperature changes.

It is recommended to perform a calibration by using a reference material from time to time in order to avoid drift of the electronics.

Irradiated Charpy specimens

The irradiated specimens under investigation are of type Charpy ISO-V (55x10x10) made from JRQ-steel (ASTM 533 B Cl. 1) by Kawasaki Steel Corporation at Mizushima Works. The chemical composition of the JRQ-material is given in Table 1. The specimens were cut from a well-specified position of a certain block.

Table 1: Chemical composition of JRQ-steel in wt-%

C	Si	Mn	P	S	Mo	Ni	Cr	Cu	V	Co	Al
0.19	0.25	1.39	0.019	0.0040	0.50	0.83	0.12	0.140	0.003	0.000	0.012

Neutron Irradiation History

The specimens suffered three different neutron irradiation histories: un-irradiated (UI), irradiated up to a certain fluence (I) and irradiated to 50% of the fluence followed by annealing 18h at 460°C and a final irradiation up to 100% fluence (IAR). This corresponds to neutron fluencies ranging from 0 up to 4.51 E^{19} n/cm^2. After irradiation, the specimens were stored for about 10 years at room temperature in the hot laboratory at PSI.

The Change of Seebeck coefficient due to neutron irradiation

To perform measurements, the specimens were taken from the hot cell and put behind a lead shielding wall where they were fixed in the TEP device. The time for applying the temperature difference and stabilising the thermoelectric output signal was chosen to 3 minutes. After read out the Seebeck coefficient, the specimens were put back into the hot cell immediately. Special attention had to be paid on the cleanness of the surface where the electrodes are in touch with the specimen. An oxide layer or other pollution leads to unreliable results. An indicator for an insufficiently clean surface is the drift of the SC signal that results in a long time to achieve stability of the output signal. We therefore had to remove the oxide layer by mechanically polishing the measured surface. Such effects might explain one part of the scatter band in the presented results.

The Seebeck coefficient of each specimen was measured at two different positions, namely at 0° (notch up) and after a rotation of 90° about the longitudinal axis (notch behind). In order to check the reproducibility of the measurements, some specimens were measured at two different days at the same position on the surface whereas an excellent reproducibility was found. Figure 1 shows the obtained Seebeck coefficients vs. neutron fluences for the irradiated (I) and also for the irradiated-annealed-irradiated (IAR) specimens. It appeared a pronounced correlation between SC and fluence. With increasing fluence the SC rises in a similar slope for both, the I- and the IAR-specimens. However, at higher fluencies it seems that the SC for the IAR-specimens is slightly lower compared with I ones. This is reflected in the slightly lower exponent of the fluence ϕ in the fit. Some indications of a saturation were also obtained in Fig. 1.

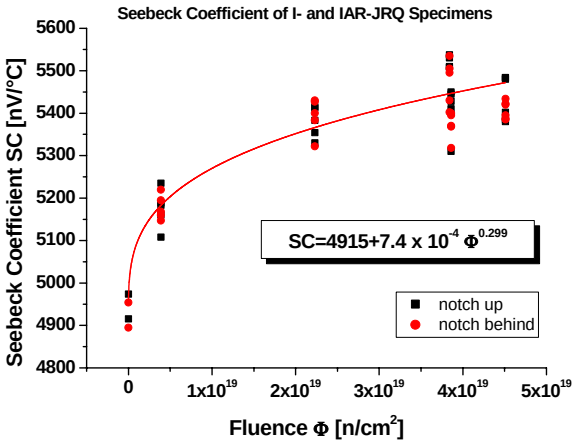

Figure 1: I- and IAR-specimens

Correlation of the TEP with neutron embrittlement

Material embrittlement due to neutron irradiation can be characterized by the shift of the Charpy energy vs. Temperature curve . T_{CNV}. This shift of the Charpy energy vs. Temperature curve was measured at energy levels of 41 J and 68 J, respectively. In Figure 2 the corresponding temperature shifts (. T_{CNV}) for the Charpy Notch V (CNV) specimens, abbreviated with . T_{41} and . T_{68}, are plotted versus the neutron fluence for the I-specimens. Finally, Figure 3 shows the . T_{CNV} as a function of the SC. The linear dependency with a slope of 7.7 nV/°C could be used for monitoring the neutron embrittlement.

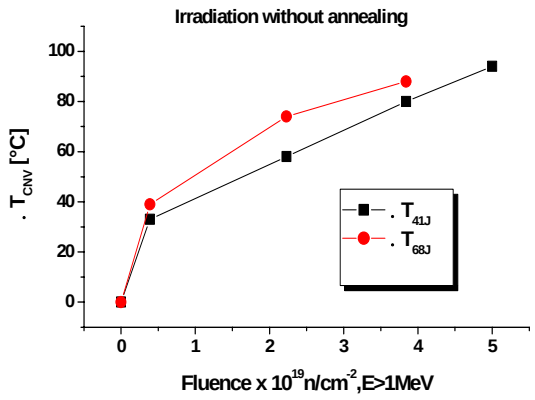

Figure 2: . T_{CNV} vs. the Fluence for I-specimens

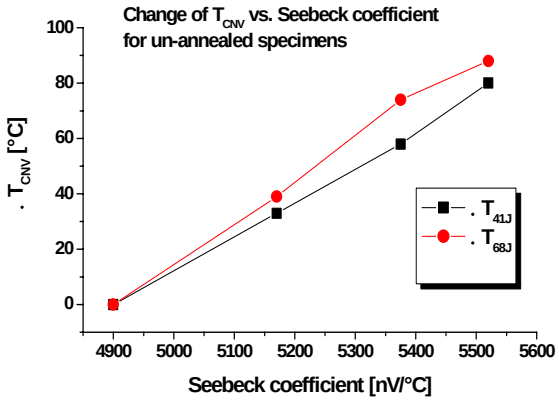

Figure 3: . T_{CNV} as a function of the SC

Measurement of Seebeck coefficient of fatigued specimens

A second important material degradation process is caused by cyclic thermomechanical strain loads, often called thermomechanical fatigue. Such loads might be the origin for the initiation and growth of cracks in cooling water tubes and surge lines [10].

The investigated fatigue specimens are made from the metastable austenitic steel X6CrNiTi18-10 according to DIN 1.4541 which corresponds to AISI 321. Before quenched in oil, the material was tempered 2h at 1040 °C . In order to achieve different strain amplitudes in the same specimen, they were made of a special hourglass shape with changing cross section (see Figure 4).

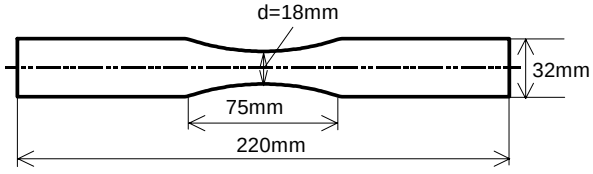

Figure 4: cross section of fatigue specimen

After fatigue by applying a cyclic strain controlled load of 2 Hz, total strain amplitude of 0.28%, at room temperature, the strain induced martensite was determined by neutron diffraction experiments at the neutron spallation source at PSI [11]. Neutron diffraction allows the non-destructive quantitative determination of martensite in the bulk of the specimen by comparing the Bragg peak for the austenitic phase with that of the martensitic peak.

The specimens were axially cut into two halves and the SC was measured on the cutting plane. The usage factor D used in Fig. 5 is defined by the relation between the number of load cycles N_i for specimen i and the averaged number of cycles needed to induce first visible micro cracks N_f ($D=N_i/N_f$). In the fatigue test this was achieved by a load drop of 5 % corresponding the maximum force load.

Thermoelectric surface scans of fatigued hourglass specimens

Due to the geometry of the specimens deformation induced martensite is located mainly in its middle part.

For specimens 2.3A (D=1, Martensite content up to 1.5 %), 2.5A (D=1, Martensite content up to 1.5 %) and 2.4A (D=0, Martensite content=0 %) we measured the SC in an interval of 3mm in order to evaluate the variation of SC in axial direction. A variation of the SC is expected due to the hourglass shaped specimen in which most of the strain induced martensite was found in the middle (at an axial distance of about 30 mm). In Figure 5 we compare the martensite distribution determined by x-ray diffraction [11] and finite element calculation with the measured SC.

The curve indicated by red dots does not change a lot with the axial position because the martensitic content in this specimen is about zero. The curve indicated by green triangles shows more or less the expected behavior, whereas the curve labeled with black squares shows some irregularities. Similar deviations from the ideal calculated distribution appeared also in the x-ray scan. As the FE calculations confirmed, the measured TEP is generated in a small location near the contact of the heating. We therefore assume that some part of the scatter can be explained by the local sensitivity of the measuring method.

Our measurements therefore proved the possibility of performing a TEP-scan over the surface of a specimen or component to gain a more complete picture of the material state as predicted by Eq. (6).

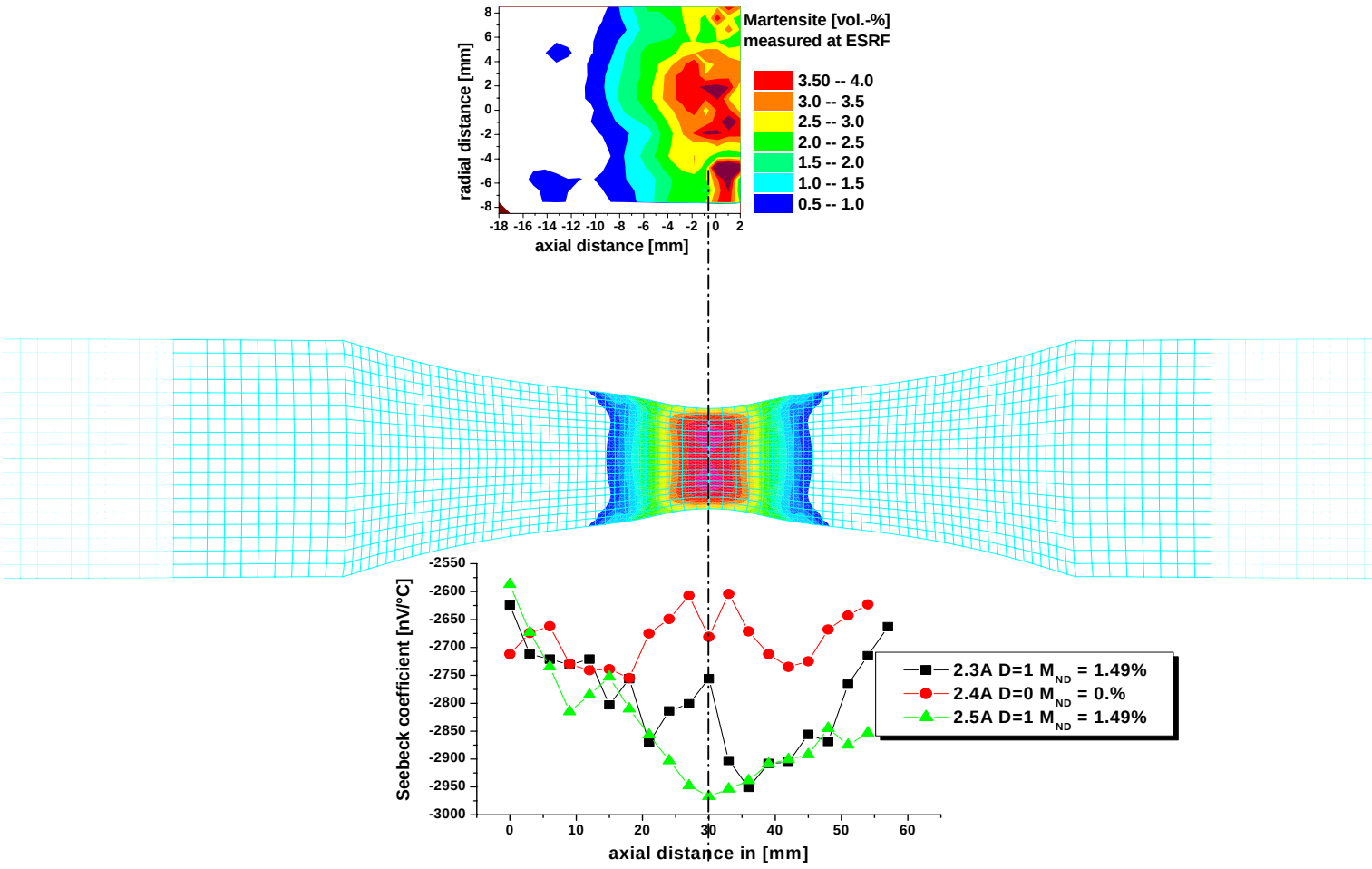

Figure 5: Comparison of martensitic strain and SC distribution

Comparison with the content of deformation-induced martensite

The variation of SC can be compared with the martensitic content, which is an indicator for the fatigue state of metastable austenitic stainless steels. A clear influence of the martensite on the SC can be seen in Figure 6. The measurements were performed on a small set of specimens and therefore the results suffer from a poor statistics. To improve the accuracy of the relation to express the SC as a function of martensite, further measurements should be performed.

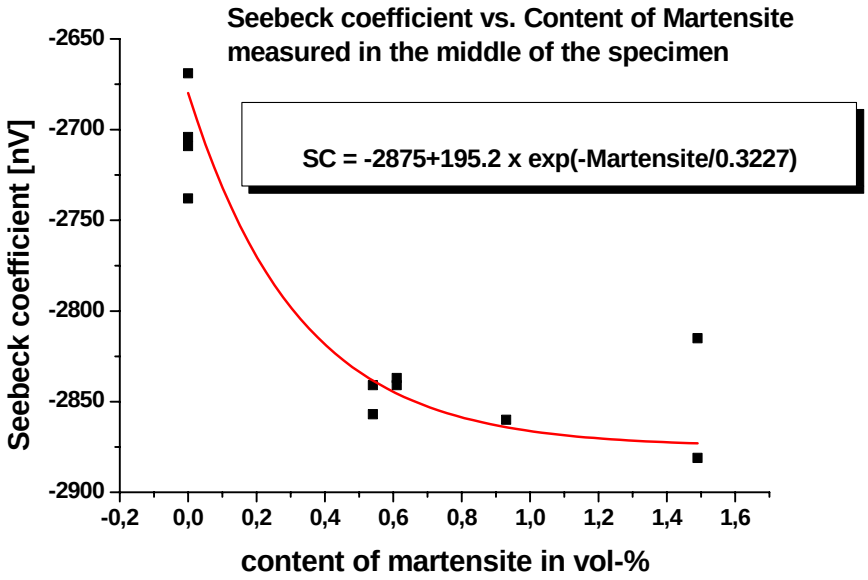

Fig. 6: Seebeck coefficient vs. martensite content in fatigued specimens X6CrNiTi18 10

DETERMINATION OF GAUGE VOLUME

As shown in Eq. (6) the generated thermoelectric voltage in a certain volume element is proportional to the temperature gradient and the local Seebeck coefficient in the corresponding volume element. If the temperature is constant over a certain part of the specimen, no contribution to the TEP will come from that part even the SC is large. To interprete the measured TEP it is therefore essential to know the size and location of varying temperature areas, especially if we are not allowed to assume a homogeneous material. For this reason extensive 3-dimensional finite element calculations were performed for our experimental arrangement.

3-D Finite Elemente Calculations

In order to analyse the temperature profile near the contact electrodes the precise 3-dimensional model takes into account the heat exchange with the ambient through the free surfaces of the Charpy specimen (Figure 7), the heat flow into the specimens at contact lines and the heat conduction in the specimen.

Only one half of the specimen was modelled with a symmetry plane in half of the depth of the specimen in order to model the physical symmetry of the problem and to get a sufficient number of elements for the required accuracy. The model is composed out of 9280 3D conduction elements in 4 element groups and 1104 convection elements laying on all outer surfaces in 4 element groups either. The finite element mesh was created with a smaller ratio of the element length around the thermocouples TC_1 and TC_2 where we will obviously find the biggest temperature gradients.

Homogeneous Neumann boundary conditions (no heat transfer normal to the plane) were applied to the symmetry plane. On the lines of thermocouples TC_1 and TC_2 Dirichlet boundary conditions were set to 25°C and 15°C, respectively in order to model the heat load. On all free surfaces we applied Cauchy boundary conditions with a heat coefficient h of 150W/m^{2}K and an ambient temperature T_0 of 20°C.

Figure 8 shows the temperature band plot on the surface of the 3D-model with a good visibility of the large gradients around the thermocouples on the surface. However, the temperature gradient in the direction of the depth is rather small.

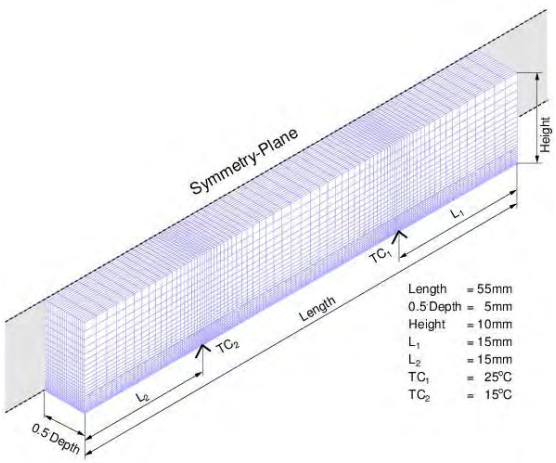

Figure 7: 3D FE-model of Charpy specimen

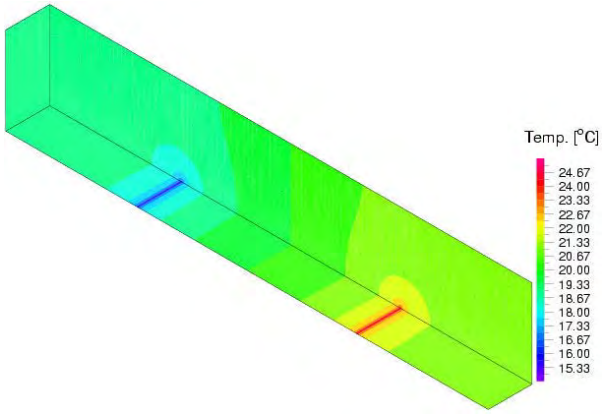

Figure 8: Temperature field on the 3D model

Outside a radius of 2.0-2.5mm of the thermocouples the temperature drops to the ambient temperature within an accuracy of 1°C. The estimated gauge volume around the two electrodes therefore is about 12 to 20 mm^3.

In the following 2 figures the temperature gradients and profiles are documented even more clearly. Figure 9 shows the temperature variation along the side of the thermocouples TC_1 and TC_2 and Figure 10 shows the temperature variation normal to the thermocouples. It is easy to recognize that outside a radius of 2.0-2.5 mm around the thermocouples the specimen is close (±1°C) to the ambient temperature of 20°C.

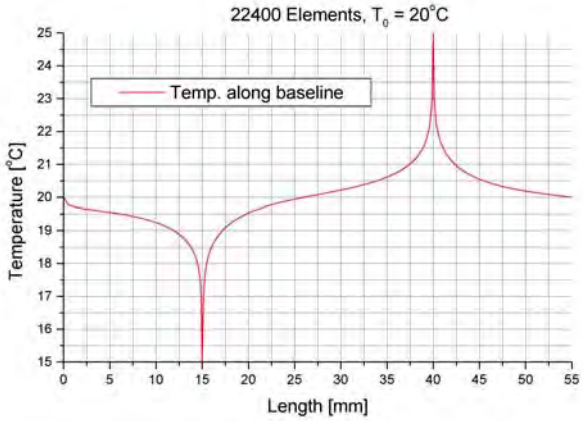

Figure 9: Temperature profile along the length of the specimen, T_0=20°C

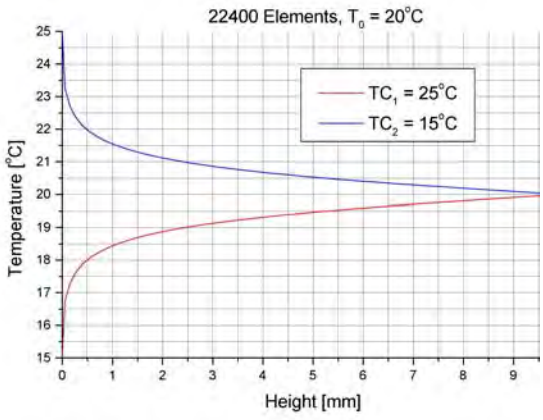

Figure 10: Temperature profile along the height of the specimen at TC_1 and TC_2, T_0=20°C

The principle of a TSM

From the obove we conclude, that it is possible to build a novel thermoelectric scanning microscope that can perform 2-dimensional or even 3-dimensional pictures of the degradation state of the specimen. The principle is as follow: A heat source is used for scanning the surface of the specimen. This can be realized with a LASER, resistant heating or another heat source that induces a hot spot in the specimen. The induced moving temperature gradient will lead to a thermoelectric power. The generated potential field can be measured with electrodes which are in contact with the specimens surface. Three components of the TEP can be measured in order to get information about the anisotropy of the SC. Dependent how the potential is measured, we will measure only the change of TEP due to inhomogeneities or the absolute TEP. To measure the x-component of the absolute TEP the potential difference between two points at different x-coordinates has to be measured, to measure the y-component of the TEP the potential difference between two points at different y-coordinates has to be measured and so on for the third component. The measured data can be stored together with the space coordinates (X,Y,Z) in order to generate a 3-dimensional plot of the SC over the surface.

A contactless heat source would have the advantage of less demanding surface preparation.

CONCLUSIONS

Measurements of the Seebeck coefficient on irradiated Charpy specimens were performed in the Hotlab at PSI. A clear correlation between neutron fluence and SC was found for the investigated JRQ-steel. The comparison of the shift in the Charpy energy vs. temperature curve, which is a measure for the material embrittlement, with the change of the SC shows a linear dependency. We therefore conclude that the change of the Seebeck coefficient can be used for monitoring the neutron irradiation induced embrittlement of RPV-steel if the initial material state is well characterized.

A significant change of the SC was also found in fatigued specimens made from austenitic steel X6CrNiTi18-10 (DIN 1.4541). The axial distribution of martensite was reflected in the SC by scanning the surface of the specimen. We mention that no cracks existed in the scanned surface. This means that fatigue of material could be detected in the pre-cracked state.

However, the SC also could vary within a component. For this reason a precise knowledge of the initial state of the material is necessary. Unfortunately, we do not know the scatter band due to material inhomogeneities of the investigated material and therefore a final jugement of the uncertainity of the TEP-methode is not possible at the moment.

A further problem is the sensitivity of the method to the surface condition. The surface has to be absolutely clean; this can be achieved by mechanically polishing.

Extensive finite element calculations have shown, that the change of SC measured is related to the small part of the specimens where the temperature gradient is applied. The calculations also have shown the influence of the ambient temperature on both, the amount of the measured TEP and the location of its generation. For inhomogeneous materials this might lead to misinterpretations of the results. However, the method has a potential to be improved by using a thermoelectric scanning microscope as proposed in this report. Such a microscope would be able to produce 3-dimensional plots in which the distribution of inhomogeneities and localized damage could be visualized. As far as we know, this method is new and might open a promising possibility for monitoring of material degradation.

Further investigations should be done in order to check the possibility of avoiding the surface problems e.g. by trying other methods of heat load (e.g. LASER) and to study the separation and quantification of influencing parameters. The application of the method to detect microstructural changes due to fatigue not only in austenitic but also ferritic steels should also be investigated.

Acknowledgement

We are grateful to Dr. J.F. Coste from EDF in F-Moret-sur-Loing cedex (France) for his support and Mr. R. Zumsteg and Mr. U. Tschanz for their assistance in performing the TEP-measurements. We also would like to thank Mr. M. Delnondedieu from EDF for his instructions and help in performing the experiment.

REFERENCES

1. A.W. Fenton, “How do thermocouples work ?” ; Nucl. En., 1980, Vol. 19, Feb., No 1, 61-63.
2. H. Ibach, H. Lüth, “Solid-State Physics“, Springer Verlag, 1995.
3. Daniel G. Sanders, “Accuracy of Type K Thermocouple Wire below 500 K: A statistical Analysis”; ISA Transactions:13 (2002-211), 1974.
4. V.A. Krivtsov, “The Stability of Microthermocouples in the 400-1200°C Temperature Range; Teploenergetika”, 20 (10) 73.76 1973.
5. D.R. Keyser, “How accurate are thermocouples, anyway ?, Age and impurities change them: how much is the question”, Instruments & Control Systems 47(3):51-54 March 1974.
6. T.G. Kollie et al., “Temperature measurement errors with type K thermocouples due to short-range ordering in Chromel”, Rev. Scl. Instrum. Vol. 46, No. 11 1975.
7. COSTE J. F., LEBORGNE J. M., MASSOUD J.P., GRISOT O., MILOUDI S., BORRELLY R.- Application of thermoelectricity to NDE of thermally aged cast duplex stainless steels and neutron irradiated ferritic steels-EPRI Workshop and NDE for damage assessment, La Jolla, 6-7 October 1997.
8. L. Debarberis, B. Acosta et al., “Assessment of Steels Ageing by Measuring the Seebeck and Thomson Effects (STEAM)”,15th World Conference on Non-Destructive Testing, 15-21 October 2000 in Rome.
9. F.Gillemot, E. Czoboly, G. Uri, “Final Database Report on IAEA CRP on Optimizing of Reactor Pressure Vessel Surveillance Programmes and their Analysis”, Vol II; IWG-LMNPP-94/7, produced by IAEA.
10. W. Kleinöder, H.-J. Golembiewski, “Monitoring for fatigue-examples for unexpected component loading, SmiRT 16 Transactions, paper 1175 (2001)
11. M. Grosse, M. Niffenegger, D. Kalkhof, “Monitoring of low-cycle fatigue degradation in X6CrNiTi18-10 austenitic steel”, Journal of Nuclear Materials 296 (2001) 305-311.